

## Molecular Physics

An International Journal at the Interface Between Chemistry and Physics

ISSN: (Print) (Online) Journal homepage: [www.tandfonline.com/journals/tmph20](http://www.tandfonline.com/journals/tmph20)

# Distribution of cage size smooths the transition from diffusive to caging in microrheology

Norma Caridad Palmero-Cruz, Sol María Hernández-Hernández, Rolando Castillo & Erick Sarmiento-Gómez

**To cite this article:** Norma Caridad Palmero-Cruz, Sol María Hernández-Hernández, Rolando Castillo & Erick Sarmiento-Gómez (26 Oct 2023): Distribution of cage size smooths the transition from diffusive to caging in microrheology, Molecular Physics, DOI: [10.1080/00268976.2023.2274505](https://doi.org/10.1080/00268976.2023.2274505)

**To link to this article:** <https://doi.org/10.1080/00268976.2023.2274505>



Published online: 26 Oct 2023.



Submit your article to this journal [↗](#)



Article views: 120






View related articles [↗](#)



View Crossmark data [↗](#)

# Distribution of cage size smooths the transition from diffusive to caging in microrheology

Norma Caridad Palmero-Cruz <sup>a</sup>, Sol María Hernández-Hernández<sup>b</sup>, Rolando Castillo <sup>c</sup> and Erick Sarmiento-Gómez <sup>a</sup>

<sup>a</sup>Departamento de Ingeniería Física, División de Ciencias e Ingenierías, Universidad de Guanajuato, León, Guanajuato, México; <sup>b</sup>Preparatoria 2 de Octubre de 1968, Benemérita Universidad Autónoma de Puebla, Puebla, México; <sup>c</sup>Instituto de Física, Universidad Nacional Autónoma de México, Ciudad de México, México

## ABSTRACT

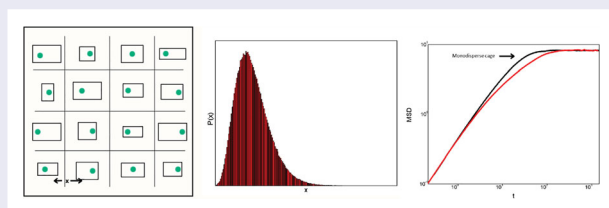
A colloidal particle undergoing Brownian motion and interacting with macromolecular structures embedded in complex fluids usually presents a diffusion regime at short times, with a diffusion coefficient related to the viscosity of the host solvent, and an intermediate regime where the mean squared displacement is found to be almost constant. This effect is attributed to the particle confinement in a cage formed by the surrounding complex fluid that hinders the motion of the tracer particle. An anomalous smooth transition that may span several decades usually characterises such a short-to-intermediate transition. In this work, this transition was studied using 1D, 2D, and 3D random walker simulations, finding that the origin of the smooth transition is a wide distribution of confining cages and the corresponding ensemble-averaged 3D mean squared displacement over all confined particles. The wider the cage distribution, the smoother the transition. Our results give the physical origin of the smooth transition, usually only discussed in terms of a distribution of relaxation times.

## ARTICLE HISTORY

Received 26 August 2023  
Accepted 17 October 2023

## KEYWORDS

Complex fluids; Brownian motion; Microrheology



## 1. Introduction

The Brownian motion of a micrometer particle in a Newtonian liquid, i.e. a memoryless, and isotropic solvent is diffusive. This means that the Mean Squared Displacement (MSD) grows linearly in time, with a diffusion coefficient that depends on the temperature, particle size, and solvent viscosity [1]. A different scenario is found when the host solvent is embedded with macromolecular structures, usually formed by the self-assembly of molecules in liquid solvents [2]. Due to the different length scales that present a complex fluid, the Brownian motion also shows time regimes associated with the interaction of the particle with the structures [3,4]. Usually, the particle samples the host solvent at short times, giving a diffusive regime. Afterward, there is a subdiffusive regime, which

is caused by hindering the motion as the particle interacts with the self-assembled structure. The subdiffusive exponent decreases as the structure is more compact and interconnected, even giving an extended plateau for cross-linked polymers and worm-like micelles formed by surfactant self-assembly [5–8]. For particles interacting with wormlike micelles in the so-called semi-dilute regime, the plateau regime extends for several decades up to a second linear regime, associated with the thermally activated process of breaking off the micelles, relaxing the stress, and as a consequence releasing the particle from the cage [5,9,10]. In all cases, the dynamics at long times is associated with more extended structures in the solution and characterised by an effective viscosity that corresponds to the zero-shear viscosity [3].

As the Brownian motion is affected by the interaction of the particle with structures of different characteristic lengths of the complex fluid, it is expected that additional information can be extracted from its MSD. An excellent example of this correlation is the technique called microrheology, where a generalised Langevin equation is used to provide a relation between the Laplace transform of the MSD of tracer particles and the complex modulus, i.e. the Fourier transform of the memory function of a step strain, thus characterising the response of the solution to a harmonic deformation [11]. This relation assumes that the local viscoelastic modulus around the particle is the same as the macroscopic viscoelastic modulus and that the Stokes relation is valid for all frequencies, thus, a homogeneous media around the particle is required. This approximation holds when the main lengths of the complex fluids are smaller than the particle size and only excluded volume interaction between particles and structures is present [12].

Microrheological techniques are now widely used to characterise the structure of complex fluids. As the probe used to sample the system is smaller than in mechanical rheometry, and considering rapid-response detection schemes such as photomultipliers in dynamic light scattering, microrheology usually is able to reach a broader range of frequencies, only limited by the inertia of the particle [3,13]. This opens the possibility of estimating the main characteristic lengths of the complex fluids, such as the persistence length, the mesh size, and the contour length, among others, from the high-frequency viscoelastic spectra. An excellent example of this realisation is the estimation of the characteristic lengths in wormlike solutions [14–17]. An interesting and common feature found in most of the systems studied using microrheology is a smooth transition from the short time regime of the MSD to a plateau, sometimes ranging several decades in time. This is usually associated with a broad spectrum of relaxation times, however, the origin of this feature in terms of the dynamics of the Brownian particle is still missing in the literature [10].

Interestingly, the dynamic scenario found in microrheological experiments of tracer particles embedded in complex fluids is also found in the colloidal glass transition, i.e. a short-time diffusion associated with small motion of colloids within the cage induced by their neighbouring particles, an intermediate regime indicative of particles being trapped in cage, and a long time diffusion related with the release of the particle from their cages due to a rearrangement of the particles [18,19].

Several approaches for simulating the Brownian motion have been developed during the last century

[1,20–22]. Among others, Brownian dynamics is particularly important as it represents a solution to the Langevin equation in the overdamped regime and can even include hydrodynamic interactions, i.e. solvent-mediated interactions [23]. In this method, a typical particle trajectory is simulated using the forces acting on the particle, and a stochastic variable is selected to fulfill the fluctuation-dissipation theorem: the computational cost is its main drawback [23]. On the other hand, a random walker simulation is computationally less expensive, and it can mimic most of the main properties of diffusive motion, such as a linear MSD and the Gaussian van Hove function self-part [24]. For this type of simulation, the step size and the time between two consecutive times are selected with simpler rules compared with a Brownian dynamics simulation, designed to give diffusive dynamics. Several applications of the random walker simulation can be found in the literature, such as in the structure of the networks in areas of sports, music, nonlinear dynamics, and stochastic chemical kinetics [25], in fields of computer science, physics, chemistry, biology [26] and also, recently it has been used in models that evaluate the effectiveness of drugs that combat coronavirus [27]. In particular, to model diffusive phenomena, it was found that a confining region where the walker is unable to escape gives a two-stage mean squared displacement: a linear regime at short times followed by a plateau that extends to larger times showing the same features of microrheological experiments, but without a long time, diffusive regime because particle is unable to escape from the confining region. Despite this similarity in the short-time to the cage transition, in the random walker simulation, such transition is sharp and can be fitted using the solution to the Langevin equation of a particle in a parabolic potential [28].

In this work, the short-to-intermediate transition was studied using random walker 1D, 2D, and 3D simulations in an ensemble of cages of different sizes. This simulates the process found in microrheology, where all particles lie in different mesh sizes, and an ensemble-averaged mean squared displacement is usually measured. This more realistic confinement method gives a smoother transition from the diffusive to the cage regime as the distribution of cage sizes becomes wider. The 1D simulation results are employed to illustrate the method used, while the 3D results were compared with experimental results. These outcomes point out that the physical origin of the smooth transition and quantify the transition's evolution depending on the width of the distribution of cage sizes. The 2D simulations results were not reported, but were used to study 2D cage distributions and are consistent with the general conclusions.

## 2. Random walker simulation

The main features of the random walker simulation used in this work are widely known [24,28] and have been explained in a previous publication [28]. Briefly, the simulation resembles a Brownian dynamic (BD) simulation, stochastically determining the position of a particle at time  $t + \Delta t$  from the position at  $t$ . In a BD simulation, the method used to determine the next step is based on the solution of the Langevin equation proposed by Ermak and McCammon [23] designed to fulfil the so-called fluctuation-dissipation theorem. In a random walker simulation, as in our case, the step size between two times,  $l$ , is chosen from a flat probability distribution,  $P(l)$ , whose width is selected to mimic a particular diffusion coefficient with the selection of time step  $\tau$ , giving a short-time diffusion coefficient  $D = \langle l^2 \rangle / 2\tau$ , where  $\langle l^2 \rangle$  is the second moment of  $P(l)$  [24]. Despite the experimental distribution is Gaussian, for the sake of simplicity, in our case  $P(l)$  was selected to be constant within the interval  $[-0.25, 0.25]$  in arbitrary units, now referred to as microns, which separated a time  $\tau = 0.1$  s, produces a MSD with a diffusion coefficient of  $0.21 \mu\text{m}^2/\text{s}$ , close to the experimental value of a colloidal suspension of  $2.8 \mu\text{m}$  confined between glass plates undergoing a quasi 2D motion. It is important to note that this value is lower than the bulk value predicted using the Stokes-Einstein relation because particles interact with the glass plates that confine the system, hindering its motion and reducing the diffusion coefficient [29]. As previously shown, the flat distribution evolves to a Gaussian distribution after a few time steps, becoming dynamically equivalent to the experiments [28]. In this scheme, external forces are complex to introduce without a bias on the step selection, but a simple confining condition can be used to restrict the motion in a desired region, which resembles most of the properties of a parabolic confining potential [24]. Interestingly the evolution of the van Hove function self-part for a free random walker, which gives the distribution probability of finding a particle at  $x$ , at time  $t$ , when the particle is initially located at  $x = 0$ , produces a Normal distribution after a few time steps, a direct consequence of the central limit theorem. Thus the random walker is dynamically equivalent to more complex BD simulations, and experimental values result after a few time steps.

As mentioned above, the random walker is based only on probabilistic rules; thus, a trapping potential cannot be included directly. Instead, confinement is introduced as rules that hinder the particle's escape from a given region or cage. This work, compares three different confining methods to contrast their properties and select the most suitable confining condition for our problem. Waiting method (a): if the next step selected from the step size

distribution is out of the cage, the walker will remain at the boundary until a step moves the walker backward. Reflecting method (b): if the next step selected from the step size distribution gives a position out of the cage, such step is performed in the opposite direction, effectively reflecting the particle back to the cage. Bouncing method (c): if the next step selected from the step size distribution is out of the cage, particles will move toward the boundary, and the remaining step length, which would come out, is performed in the opposite direction, effectively returning to the cage.

The 1D, 2D, and 3D simulations were performed in an ensemble of cages with no correlation between the size selection of their sides. The size  $z$  of the confining region was randomly selected using two distributions: a Normal distribution  $z_N$ , generated using the Box-Muller transformation [30]

$$z_N = \mu + \sigma \chi, \quad (1)$$

where  $\mu, \sigma$  are the mean and the standard deviation, respectively, and

$$\chi = \sqrt{-2 \ln(\epsilon_1)} \sin(2\pi\epsilon_2), \quad (2)$$

with  $\epsilon_1, \epsilon_2$  two pseudo-random numbers uniformly distributed in the interval  $[0, 1]$ .  $\chi$  is the inverse transformation of our original independent variables  $\epsilon_1$  and  $\epsilon_2$ , which results is a random variable with a standard normal distribution [31]. Additionally, a Log Normal distribution  $z_{LN}$  (LN) was also used to determine the size of the confining region. It was found that this distribution fits the mesh size distribution in hydrogels samples, as determined by a combination of rheology and NMR [32]. Sampling such distribution can be done by considering that the cumulative distribution function of the LN distribution is similar to the case of a Normal distribution but with a variable change  $z_{LN} = \ln(z_N)$ . Thus, this method follows the same protocol as the Normal distribution, taking the output's exponential value. However, care must be taken to correctly choose the parameters  $\mu$  and  $\sigma$  as in the new distribution; they have different meanings. Moreover, depending on  $\sigma$ , different regimes can be defined, with different evolution of the distribution on its parameters, and thus a proper selection of  $\mu$  and  $\sigma$  must be made to give a similar distribution as in the Normal case [33]. However, increasing  $\sigma$  is generally associated with a distribution with a long tail and thus can be used to extend the results obtained using a Normal distribution if  $\mu$  is properly selected.

Finally, in both cases, we considered  $n = 150$  confined random walkers with  $10^6$  steps generated, and the ensemble and time-averaged total mean squared displacement was calculated up to  $10^5$  lag steps, thus corresponding to  $10^4$  seconds.

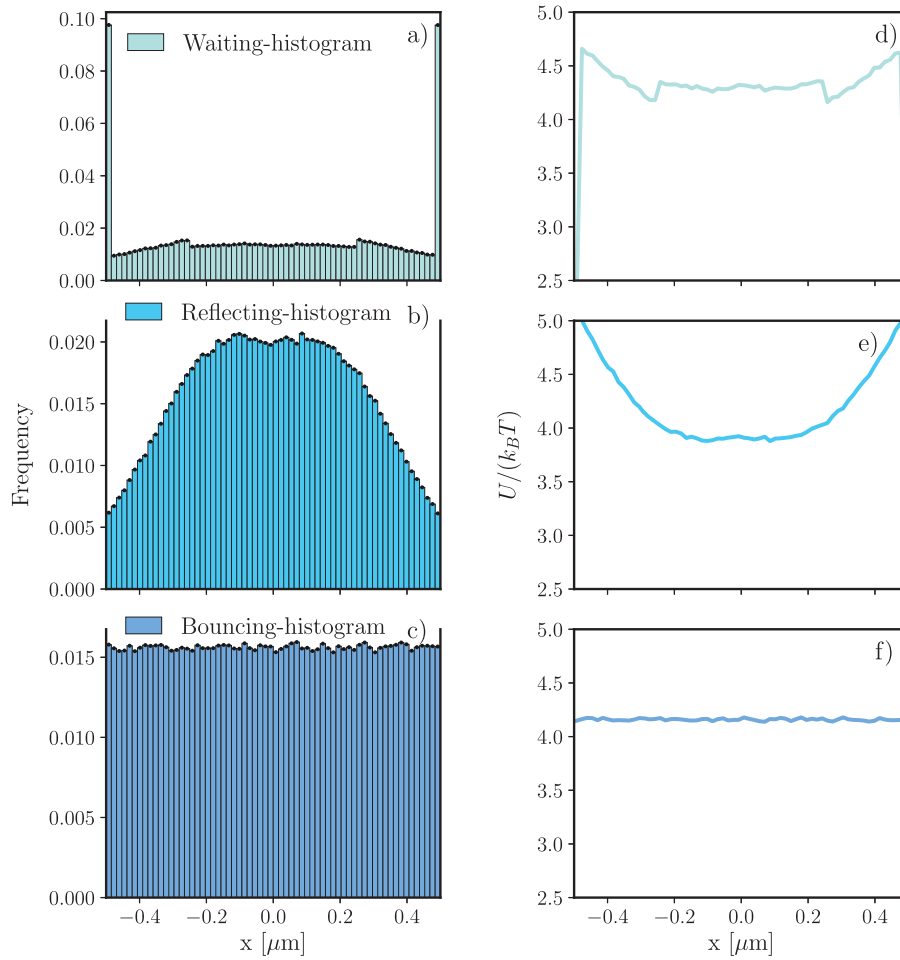


**Figure 1.** Position distributions (left column) and their corresponding effective potential (right column) for a random walker in a 1D cage of size  $1 \mu\text{m}$  for different confining methods: (a) Waiting method (b) Reflecting method, and (c) Bouncing method.

### 3. Results

1D simulations are used to illustrate the behaviour that appears when different confining methods are used. The position distribution within a cage was calculated for a fixed cage size of  $z = 1 \mu\text{m}$  to compare the statistical properties derived from the three confining methods described above. In equilibrium, the position distribution follows a Boltzmann distribution for the random walkers, and the effective potential,  $U(x)$ , acting on them, can be extracted from  $P(x) \sim \exp(-U(x)/(k_B T))$ , where  $x$  is the 1D position of the walker. As expected, the Waiting method (a) presents two peaks at the cage's border, see Figure 1(a). The particle remains in the boundary until a step moves it backward. This distribution resembles an attraction between the particle and the cage wall. The position distribution decreases as the particle position is close to the boundary, within a region separated from the wall by exactly a step size. Close to the boundary, any sufficiently big step selected from the step distribution will produce the particle to be immediately back-reflected,

reducing the probability of finding the particle close to the boundary. From the position distribution, the effective potential is calculated and shown in Figure 1(d), where the two minima at the boundary are present. The potential is found to have several discontinuities associated with irregularities in the position distribution. The reflecting condition also presents a region with lower values in the position distribution, which is separated from the wall by a step size as before. However, no peak is found at the boundary for the position distribution, as shown in Figure 1(b), giving an effective repulsive interaction close to this boundary, as shown in Figure 1(e) for the effective potential. A region as that present in the reflective condition is completely absent in the Bouncing method (c), which produces a constant position distribution within the cage and, consequently, a flat potential, as shown in Figure 1(c,f), and thus resembles a confining cage with impenetrable walls. It is interesting to note that the same position distribution is obtained when periodic boundary conditions are applied to a random walker and the position is reduced to a single unit cell.



Before selecting any particular confining method, we analyse the most important dynamical property, the ensemble-averaged MSD,  $\langle \Delta \vec{r}(t)^2 \rangle$ , of  $n$  walkers at time  $t$ ,

$$\langle \Delta \vec{r}(t)^2 \rangle = \frac{1}{n} \sum_{i=1}^n (\vec{r}_i(t) - \vec{r}_i(0))^2, \quad (3)$$

where  $\vec{r}_i(0)$  and  $\vec{r}_i(t)$  are the referential position and the position at time  $t$  of the  $i$ th particle, respectively. Figure 2 shows the total MSD for a cage size of  $z = 1 \mu\text{m}$  for the confining methods under study. In all cases, two regimes were found: diffusion at short times associated with the random motion of the particle within the cage and a plateau region at long times; walkers are unable to escape from the cage. Despite having the same cage size, the methods reach different values of the MSD for long times. The higher MSD values were found in the Waiting method (a) because the random walker has a higher probability of being found close to the boundary. The sticking condition at the boundary seems to affect the short-time diffusion coefficient, having a smaller value than the other methods, as there is a possibility of a zero displacement between two consecutive times precisely at the boundary. In contrast, the smaller value of a plateau was found on the Reflecting method (b), presumably due to the effective repulsive potential close to the boundary associated with such confining method having a smaller probability of finding the particle close to the boundary. The case with a plateau value in-between the two mentioned methods, with no particularities at short times, was the Bouncing method (c). Thus, it was used in further simulations as it resembles a flat effective potential, as shown in the position size distribution in Figure 1(c) and the corresponding effective potential Figure 1(f).

The dynamics presented here, no matter the kind of confinement used, reflect the same time regimes as in particles trapped in a parabolic potential, as in optical tweezers, and can be determined using the solution to the Langevin equation with negligible inertia, with slightly different optical stiffnesses to reach different values of the MSD in the plateau [34]. Equivalently, we can also use the Smoluchowski formalism to understand the time regimes shown. The Smoluchowski equation for a particle trapped in a parabolic potential can be written in 1D in the following form

$$\frac{\partial \Psi}{\partial t} = \frac{\partial}{\partial x} \left[ \frac{k_B T}{\xi} \frac{\partial \Psi(x, t)}{\partial x} + \frac{k}{\xi} (x \Psi(x, t)) \right], \quad (4)$$

where  $k$  is the constant of the parabolic potential and  $\xi$  is the friction coefficient. For a constant diffusion coefficient  $D = k_B T / \xi$  and considering that the probability distribution vanishes exponentially, its solution for the

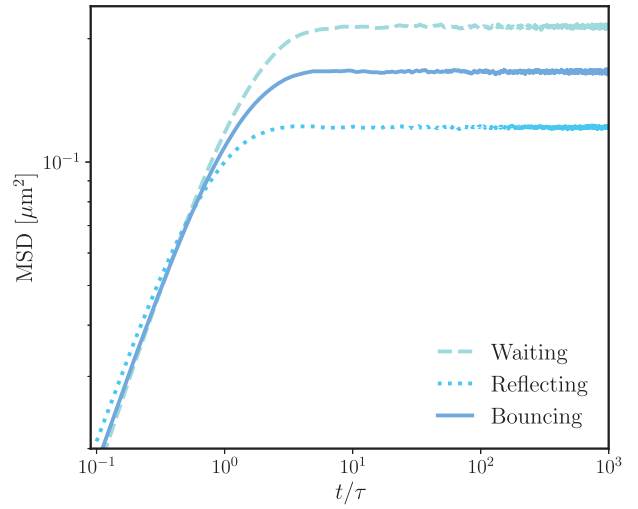


**Figure 2.** Total mean squared displacement for the 1D random walker for the different confining methods used in this work and for the same cage size  $1 \mu\text{m}$ .

initial condition  $\Psi(x, t = 0) = \delta(x - x_0)$ , where  $\delta$  is the delta function, is given by:

$$\Psi(x, t) = \frac{1}{\sqrt{2\pi \left(\frac{\xi D}{k}\right) \left(1 - \exp\left[-2\frac{k}{\xi}t\right]\right)}} \times \exp\left\{-\frac{\left(x - x_0 \exp\left[-\frac{k}{\xi}t\right]\right)^2}{2 \left(\frac{\xi D}{k}\right) \left(1 - \exp\left[-2\frac{k}{\xi}t\right]\right)}\right\}, \quad (5)$$

from which the MSD can be calculated, giving  $\langle (x - x_0)^2 \rangle = \left(\frac{\xi D}{k}\right) \{1 - \exp[-2\frac{k}{\xi}t]\}$ . From here, for short-times the MSD gives  $\langle (x - x_0)^2 \rangle = 2Dt$  (linear time dependence); for intermediate times  $\langle (x - x_0)^2 \rangle = 2\delta^2 \{1 - \exp[-2\frac{k}{\xi}t]\}$  defining  $2\delta^2 = \frac{\xi D}{k}$ , which is similar to what is observed in Figure 2, and for long times the RMS reduces to one constant  $\langle (x - x_0)^2 \rangle = 2\delta^2$  (a plateau), which is a measure of the size of particle's displacement around a mean position; in 3D in a homogeneous media,  $\langle (x - x_0)^2 \rangle = 6\delta^2$ . Thus, this formalism reproduce exactly the same time regimes found in the simulations.

Using the Bouncing method (c), which gives a flat distribution of positions within the confining cage, we now move to compute the statistical properties of an ensemble of confined 2D and 3D random walkers whose cage size is selected from a given distribution. Despite this, the distribution of confining cage areas (2D) and cage volumes (3D) are quite different, also having an important dependence on the parameters of the cage size distribution, as shown in the inset of Figure 3 (left panel). Small widths give an almost Normal distribution of confining areas and volumes, as seen in the main part of Figure 3

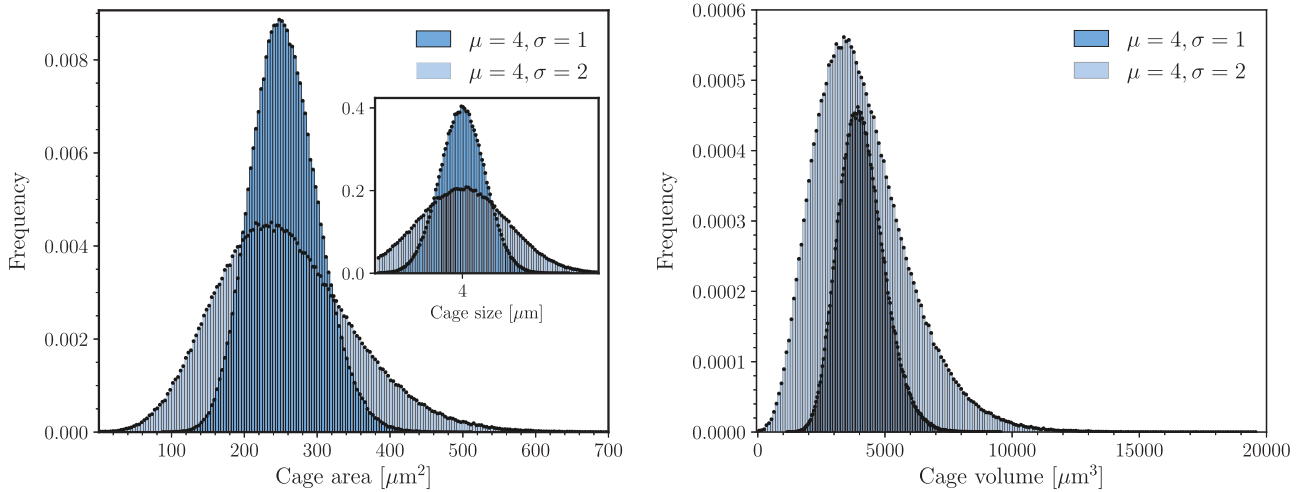


**Figure 3.** Comparison of the distribution of cage areas (left panel) and cage volumes (right panel) with  $\mu = 4$ ,  $\sigma = 1$ , and  $\sigma = 2$ , respectively. Inset in left: shows the cage size distribution for the same parameters as in the main part of the figure.

(left panel and right panel respectively), but the distribution evolves with a tail at more extended areas and cage volumes when increasing  $\sigma$ . This is expected to affect the ensemble average MSD, as shown below for the 3D case.

Before analysing any dynamical property, we first examine the shape of the ensemble-averaged position distribution for the case where a distribution of cage sizes is employed for the case of the Bouncing method (c) and compare it with the result shown before in Figure 1 where the 1D-walker is confined in a cage of constant size. The Bouncing confinement condition gives a flat position distribution at each cage, as shown in Figure 1(c). However, in the following lines, we will quantify properties averaged over several random walkers, each randomly selected from a normal distribution of cages. The normalised histogram of the position averaged over all walkers is shown in Figure 4, finding a distribution similar to a normal distribution but with an almost flat region close to  $x=0$ . For this calculation, 500 cage sizes were randomly selected following the rules motioned above, with  $\mu = 5$  and  $\sigma = 1$ . The central and almost flat part of the distribution is attributed to the smaller cages, between 2 and 3  $\mu\text{m}$  in size, also flat within this range, whereas the overall shape is the consequence of the averaging of independent samples with finite variance and thus similar to a normal distribution.

Once the behaviour of the different assemblies has been discussed. Our next step was to perform 3D simulations in an ensemble of cages with a given size distribution for the case of Bouncing confinement. Figure 5 shows the MSD for particles confined in cages with a mean size between a  $\mu = [5, 10]$  and  $\sigma = [0.25, 7]$ . In all the cases, 150 simulations were run, where in each simulation the three sizes of the confining cage were independently selected using the normal generator indicated

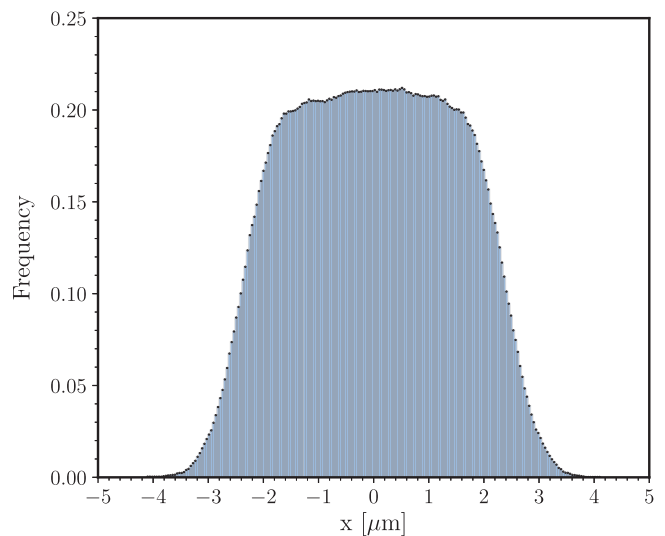


**Figure 4.** Total position distribution of an ensemble of 500, 1D-random walkers confined in cages selected from a size Gaussian distribution with a  $\mu = 5$  and  $\sigma = 1$  for the case of Bouncing confinement.

in the Section 2. A diffusive regime is always found at short times no matter the properties of the position distribution, consistent with the same diffusion coefficient for a free particle, which is related to the free diffusion of the walkers inside a cage. At long times it is also found a plateau regime no matter the width of the distribution. Notable, the MSD deviates from diffusion and reaches the plateau at different times depending on the width of the cage distribution. When comparing the MSDs with the same  $\mu$  values, broader distributions are associated with a smoother transition from the linear to the plateau regime, taking more time to reach such a regime. A mostly monodisperse 3D simulation with

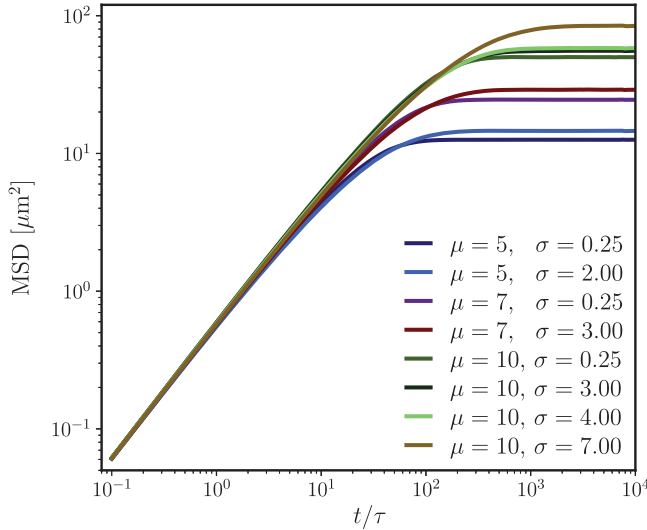


**Figure 5.** Ensembled averaged total mean squared displacement for 3D random walkers confined in a distribution of cages with  $\mu = [5, 7, 10]$  and  $\sigma = [0.25, 2, 3, 4, 7]$ .

$\mu = 5$  and  $\sigma = 0.25$ , usually requires only a decade to reach the transition, whereas the sample with  $\mu = 10$  and  $\sigma = 7$  requires approximately two decades to reach the cage regime. Exactly this smooth transition is found in microrheological experiments [14–17]. The results found here indicate that the origin of this transition is related to the polydispersity of the confining cages, as it is expected to be present in complex fluids made of cylindrical giant micelles. Fluctuations in the supramolecular structures and thermal motion define the fluid stress relaxation and the cage size that undoubtedly corresponds to the mean value of the fluctuating cages shown by our simulations.

To quantify the features of results presented in Figure 5, the total MSD is fitted to a model curve partially proposed by Bellour et al. [10] to describe the MSD of colloidal particles embedded in solutions of giant cylindrical micelles forming a network. These authors supposed that each colloidal particle is harmonically bound and executes Brownian motion around a stationary mean position. They obtained an expression for the MSD similar to that used in the case of particles trapped by optical tweezers:

$$\langle \Delta r(t)^2 \rangle = 6\delta^2 \left[ 1 - e^{-\left(\frac{D}{\delta^2}t\right)^\alpha} \right]^{1/\alpha}, \quad (6)$$

where  $D$  is the short-time diffusion coefficient,  $6\delta^2$  is the value of the MSD at the plateau, and  $\alpha$  is the smooth parameter for the short-time to plateau transition. This initially proposed model curve includes an additional term required to display a second linear diffusive at long times, which is not required in our case. Equation (6) with an  $\alpha = 1$  corresponds to the solution to the Langevin

equation for a particle in a parabolic potential, as shown before [34]. However, in microrheological experiments made in WLMs, values of  $\alpha$  between 0.25 and 0.3 are commonly found [10,16,35]. Usually, this model fits well the experimental MSD data. Using the Mason-Weitz formula, the mesh size gives  $\xi = \pi a(6\delta^2)$  where  $a$  is the particle radius.

In Figure 6 (left panel), we show the behaviour of  $\alpha$  for different  $\sigma_{(i)}$  value. For a better comparison, the standard deviation  $\sigma_{(i)}$  was normalised with its corresponding  $\mu$  values. For a distribution width of zero,  $\alpha$  is found to be close to 0.85, and it decreases monotonically to a value close to 0.55 for broader size distributions evaluated using the normal distribution. This trend agrees with our finding: the wider the distribution of confining cages, the smoother the transition to the plateau regime. Remarkably, the MSD of a trapped particle in a parabolic potential, experimentally realised using optical tweezers, can be fitted to Equation (6) with a value near to 0.9, which is close to our case of a monodisperse cage [34], which is in agreement that  $\sigma$  defines the size of the cage.

Another key parameter is the value of the MSD at the plateau ( $6\delta^2$ ), see Figure 6 (right panel). The value of the plateau always remains in the same order of magnitude no matter the distribution width used. Major changes occur as the mean value of the distribution is modified, as expected, due to the different confinement associated with each cage size. The only difference is the transition time between the short-time diffusive and plateau regimes at intermediate times. A linear fit of the short and plateau regimen (in log scale) was made to quantify this transition time, identifying the cross time  $\tau_c$  as the interception between both linear fittings. Figure 7 shows our results. The  $\tau_c$  values present significant variations, close to an order of magnitude between the zero width and the broadest distribution used here. Comparing Figures 6 and 7 we can note that the behaviour of  $\tau_c$  relative to  $\sigma_{(i)}/\mu$  is similar to the  $6\delta^2$ .

As reported in the literature, the  $\alpha$  parameter associated with microrheological experiments is found to be between 0.25 and 0.3 [10,16,35], still far away from our simulation results. Nevertheless, the trend of this parameter  $\alpha$  with the cage distribution width is correct. To better elucidate the origin of this trend, a comparison with microrheological experiments can be made by fitting the MSD to the model curve proposed by Bellour, Equation (6), but without including the  $\alpha$  parameter. This fitting allows us to better visualise the evolution of the MSD in terms of normalised time  $t/\tau$  where  $\tau = \delta^2/D_0$ , and the normalised MSD  $\langle \Delta r^2 \rangle / (6\delta^2)$ . For comparison purposes, the same fitting was applied to microrheological data from the mixture TDPS-SDS surfactants and brine, which forms a solution with worm-like micelles,



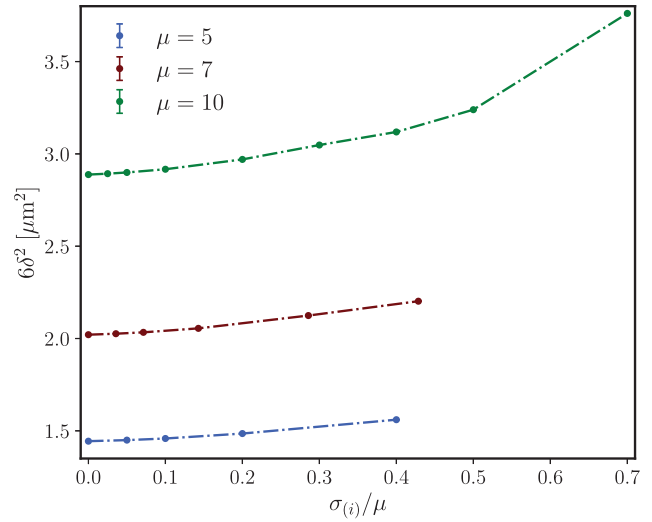
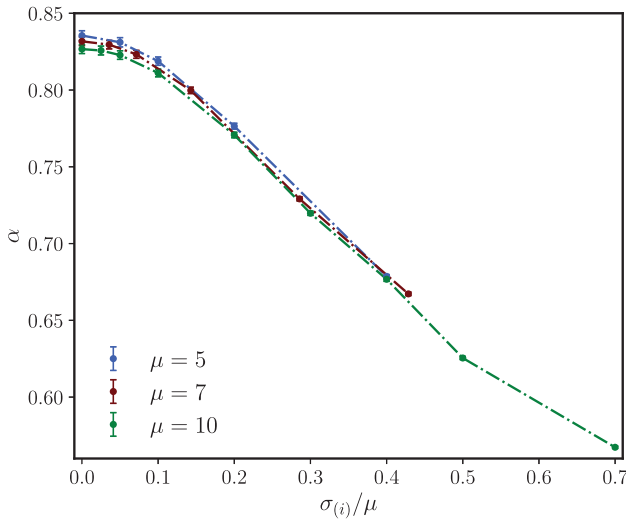


**Figure 6.** The  $\alpha$  (left panel) and  $6\delta^2$  (right panel) parameters of the proposed fitting model in Equation (6) for different  $\sigma_{(i)}$  values normalised with  $\mu$ .

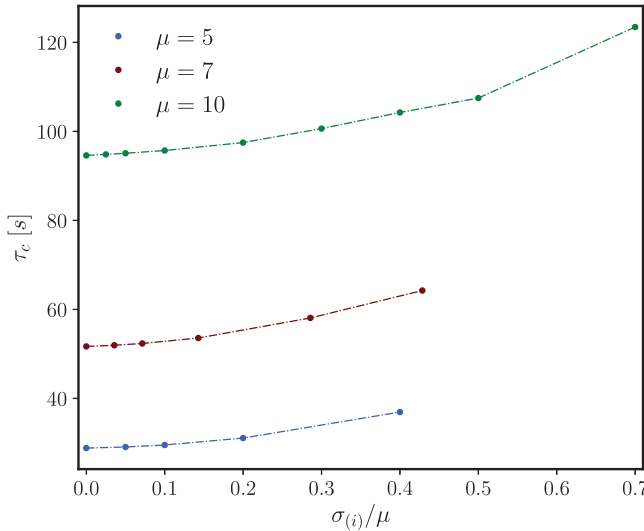


**Figure 7.** Transition  $\tau_c$  between the short time diffusion regime and the plateau region at intermediate times for different  $\sigma_{(i)}$  values normalised with  $\mu$ .

as reported in [16]. We will focus our attention in the case of a total concentration of 46 mW, a TDPS/SDS ratio concentration  $R = 0.55$  and NaCl concentration of 0.4M. From the 3D simulation counterpart, the case for  $\mu = 10$  and  $\sigma = 0, 3$  and 7 were analysed. The results are shown in Figure 8. As expected, all curves share the same diffusion to plateau transition, but the transition regime evolves differently: increasing the width of the distribution gives a smoother transition, but more importantly, the trend when increasing the width of the distribution is in the direction of the microrheological WLM experiments. This behaviour suggests that a wider distribution of cages is required to get a value of  $\alpha$  as

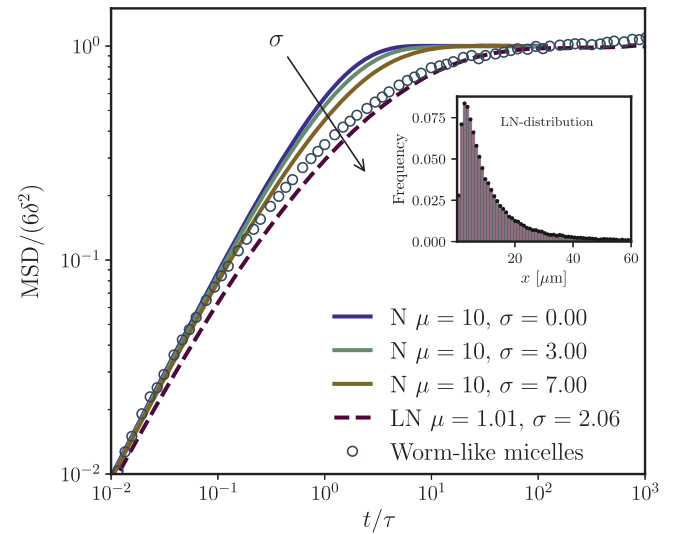


**Figure 8.** Normalized mean squared displacement,  $\text{MSD}/(6\delta^2)$  computed for 3D simulations as a function of the normalised time,  $t/\tau$  for particles in an ensemble of cages whose size is selected from a Normal distribution (labeled as N) and a Log Normal distribution (labeled as LN) at the  $\mu$  and  $\sigma$  parameters indicated in the legend. The microrheological experimental data for a worm-like micelle solution coming from [16] are also shown.

small as in the experiments; however, we are unable to increase this value further as it would give negative values for the cage size. This also indicates that a different model for the distribution of cage sizes is required. To further push the smoothness of the transition, an LN distribution was also explored for a particular case, namely  $\mu = 1.01$  and  $\sigma = 2.06$ , whose distribution is shown in the inset of Figure 8. The MSD associated with this distribution is shown in Figure 8 as a dashed line, finding a better agreement with the microrheological case and an

$\alpha$  value of 0.36, closest to those reported previously in microrheological experiments [35]. Interestingly the LN distribution resembles the mesh size distribution determined by a combination of low-field NMR and mechanical rheology in an interpenetrating polymer network hydrogel, whose structure is expected to share similarities with the self-assembled system that forms worm like micelles [32]. Thus, we can conclude that an asymmetric distribution with a higher probability of finding big cage sizes is required to reproduce the smooth transition between the short-time and plateau regimes in microrheological experiments. Closely related with this finding, the mean square displacement of colloids near the glass transition, at a volume fraction of  $\phi = 0.583$ , can also be fitted to the Equation (6), with  $\alpha \approx 0.27$  (see [19] for experimental data obtained from dynamic light scattering) and thus also presents the same anomalous transition. Then we can also speculate that, in this case, the relaxation distribution of the so-called beta relaxation is also related with the distribution of confining cages where each particle is sampling when undergoing Brownian motion.

#### 4. Conclusions

In this work, we analyse the dynamics of an ensemble of 1D, 2D and 3D random walkers confined in impenetrable cages whose sizes were chosen randomly following a Gaussian distribution. An averaging process was selected to simulate microrheological experiments in which colloidal tracers interact with complex fluids embedded with threadlike structures, such as wormlike micelles formed by the self-assembly of surfactant molecules. An important feature of these experiments is a smooth transition from short-time diffusion to a plateau at intermediate times related to the confinement of the tracer particle when interacting with complex fluids. Our results indicate that the 3D simulations can reproduce this smooth transition's experimental feature, with a parameter that increases as the cage size distribution becomes broad. However, a more complex distribution is required to obtain a smooth parameter closer to that used in the experiments, such as a log normal distribution. Interestingly this distribution also resembles the distribution of mesh sizes reported in the literature for a hydrogel, whose structure is expected to share similarities with worm-like micelle systems. Our findings corroborate that the origin of the anomalous smooth transition in the microrheology of worm-like micelles is related to the distribution of confining cages attributed to the random placement of threat-like structures that hinders the motion of the tracer particle.

#### Disclosure statement

No potential conflict of interest was reported by the author(s).

#### Funding

Financial support (CONACyT grants: A1-S-15587, A1-S-9098, Ciencia de Frontera N 102986, and DGAPAUNAM grant IN 106321) is gratefully acknowledged. N. C. P.-C. acknowledge support by CONACyT graduate scholarship No. 1047267.

#### ORCID

Norma Caridad Palmero-Cruz  <http://orcid.org/0000-0002-7706-0592>

Rolando Castillo  <http://orcid.org/0000-0001-6331-0311>

Erick Sarmiento-Gómez  <http://orcid.org/0000-0001-6130-4161>

#### References

- [1] J.K.G. Dhont *An Introduction to Dynamics of Colloid* (Elsevier, Amsterdam, 1996).
- [2] I.W. Hamley, *Introduction to Soft Matter* (John Wiley and Sons, Chichester, 2008).
- [3] E.M. Furst and T.D. Squires, *Microrheology* (Oxford University Press, New York, 2017).
- [4] F. MacKintosh and C. Schmidt, *Curr. Opin. Colloid. Interface. Sci.* **4** (4), 300–307 (1999). doi:10.1016/S1359-0294(99)90010-9
- [5] F. Cardinaux, L. Cipelletti, F. Scheffold and P. Schurtenberger, *Europhys. Lett.* **57** (5), 738 (2002). doi:10.1209/epl/i2002-00525-0
- [6] B.R. Dasgupta and D.A. Weitz, *Phys. Rev. E* **71**, 021504 (2005). doi:10.1103/PhysRevE.71.021504
- [7] T.H. Larsen and E.M. Furst, *Phys. Rev. Lett.* **100**, 146001 (2008). doi:10.1103/PhysRevLett.100.146001
- [8] E. Sarmiento-Gomez, I. Santamaría-Holek and R. Castillo, *J. Phys. Chem. B* **118** (4), 1146–1158 (2014). doi:10.1021/jp4105344
- [9] M.E. Cates and S.J. Candau, *J. Phys.: Condens. Matter* **2** (33), 6869 (1990).
- [10] M. Bellour, M. Skouri, J.P. Munch and P. Hébraud, *Eur. Phys. J. E* **8**, 431–436 (2002). doi:10.1140/epje/i2002-10026-0
- [11] T.G. Mason and D.A. Weitz, *Phys. Rev. Lett.* **74**, 1250–1253 (1995). doi:10.1103/PhysRevLett.74.1250
- [12] T.G. Mason, *Rheol. Acta.* **39** (4), 371–378 (2000). doi:10.1007/s003970000094
- [13] Q. Xia, H. Xiao, Y. Pan and L. Wang, *Adv. Colloid. Interface. Sci.* **257**, 71–85 (2018). doi:10.1016/j.cis.2018.04.008
- [14] N. Willenbacher, C. Oelschlaeger, M. Schopferer, P. Fischer, F. Cardinaux and F. Scheffold, *Phys. Rev. Lett.* **99**, 068302 (2007). doi:10.1103/PhysRevLett.99.068302
- [15] J. Galvan-Miyoshi, J. Delgado and R. Castillo, *Eur. Phys. J. E* **26** (4), 369–377 (2008). doi:10.1140/epje/i2007-10335-8
- [16] E. Sarmiento-Gomez, D. Lopez-Diaz and R. Castillo, *J. Phys. Chem. B* **114** (38), 12193–12202 (2010). doi:10.1021/jp104996h
- [17] A. Tavera-Vazquez, N. Rincon-Londono, R.F. Lopez-Santiago and R. Castillo, *J. Phys.: Condens. Matter* **34** (3), 034003 (2021).

- [18] G.L. Hunter and E.R. Weeks, *Rep. Prog. Phys.* **75** (6), 066501 (2012). doi:[10.1088/0034-4885/75/6/066501](https://doi.org/10.1088/0034-4885/75/6/066501)
- [19] W. van Meegen, T.C. Mortensen, S.R. Williams and J. Müller, *Phys. Rev. E* **58**, 6073–6085 (1998). doi:[10.1103/PhysRevE.58.6073](https://doi.org/10.1103/PhysRevE.58.6073)
- [20] M. Allen, M. Allen, D. Tildesley and D. Tildesley, *Computer Simulation of Liquids* (Oxford Science Publ, New York, 1989).
- [21] S. Herrera-Velarde, E.C. Euán-Díaz, F. Córdoba-Valdés and R. Castañeda-Priego, *J. Phys.: Condens. Matter* **25**, 325102 (2013).
- [22] M. Fixman, *Macromolecules* **19** (4), 1195–1204 (1986). doi:[10.1021/ma00158a042](https://doi.org/10.1021/ma00158a042)
- [23] D.L. Ermak and J.A. McCammon, *J. Chem. Phys.* **69** (4), 1352–1360 (1978). doi:[10.1063/1.436761](https://doi.org/10.1063/1.436761)
- [24] S. Chandrasekhar, *Rev. Mod. Phys.* **15**, 1–89 (1943). doi:[10.1103/RevModPhys.15.1](https://doi.org/10.1103/RevModPhys.15.1)
- [25] T.J. Perkins, E. Foxall, L. Glass and R. Edwards, *Nat. Commun.* **5** (2014). doi:[10.1038/ncomms6121](https://doi.org/10.1038/ncomms6121)
- [26] F. Xia, J. Liu, H. Nie, Y. Fu, L. Wan and X. Kong, *IEEE Trans. Emerg. Topics Comput.* **4** (2), 95–107 (2020). doi:[10.1109/TETCI](https://doi.org/10.1109/TETCI)
- [27] L. Shen, F. Liu, L. Huang, G. Liu, L. Zhou and L. Peng, *Comput. Biol. Med.* **140**, 105119 (2022). doi:[10.1016/j.combiomed.2021.105119](https://doi.org/10.1016/j.combiomed.2021.105119)
- [28] D. Pérez-Guerrero, J.L. Arauz-Lara, E. Sarmiento-Gómez and G.I. Guerrero-García, *Front. Phys.* **9**, 635269 (2021).
- [29] M. De Corato, F. Greco, G. D’Avino and P.L. Maffettone, *J. Chem. Phys.* **142** (19), 194901 (2015). doi:[10.1063/1.4920981](https://doi.org/10.1063/1.4920981)
- [30] G.E.P. Box and M.E. Muller, *Ann. Math. Stat.* **29** (2), 610–611 (1958). doi:[10.1214/aoms/1177706645](https://doi.org/10.1214/aoms/1177706645)
- [31] D.G.A. Addaim and A.A. Madi, *Int. J. Comput. Sci. Math.* **9** (3), 287–297 (2018). doi:[10.1504/IJCSM.2018.093153](https://doi.org/10.1504/IJCSM.2018.093153)
- [32] L. Pescosolido, L. Feruglio, R. Farra, S. Fiorentino, I. Colombo, T. Coviello, P. Matricardi, W.E. Hennink, T. Vermonden and M. Grassi, *Soft Matter* **8**, 7708–7715 (2012). doi:[10.1039/c2sm25677k](https://doi.org/10.1039/c2sm25677k)
- [33] M. Romeo, V. Da Costa and F. Bardou, *Eur. Phys. J. B* **32** (4), 513–525 (2003). doi:[10.1140/epjb/e2003-00131-6](https://doi.org/10.1140/epjb/e2003-00131-6)
- [34] G. Pesce, G. Volpe, O.M. Maragó, P.H. Jones, S. Gigan, A. Sasso and G. Volpe, *J. Opt. Soc. Am. B* **32** (5), B84–B98 (2015). doi:[10.1364/JOSAB.32.000B84](https://doi.org/10.1364/JOSAB.32.000B84)
- [35] N. Rincón-Londoño, A. Tavera-Vázquez, C. Garza, N. Esturau-Escofet, A. Kozina and R. Castillo, *J. Phys. Chem. B* **123** (44), 9481–9490 (2019). doi:[10.1021/acs.jpcc.9b07276](https://doi.org/10.1021/acs.jpcc.9b07276)